

1 **Role of time-averaging of eddy covariance fluxes on water use efficiency** 2 **dynamics of Maize crop**

3 Arun Rao Karimindla, Shweta Kumari, Saipriya SR, Syam Chintala*, and BVN Phanindra
4 Kambhammettu

5 Department of Civil Engineering, Indian Institute of Technology Hyderabad, Telangana, India.

6 *Corresponding author: E-Mail: ce22resch11012@iith.ac.in; Tel: +91 7997014429

7 **Abstract**

8 Direct measurement of carbon and water fluxes at high frequency makes eddy
9 covariance (EC) as the most preferred technique to characterize water use efficiency (WUE).
10 However, reliability of EC fluxes is largely hinged on energy balance ratio (EBR) and inclusion
11 of low-frequency fluxes. This study is aimed at investigating the role of averaging period to
12 represent EC fluxes and its propagation into WUE dynamics. Carbon and water fluxes were
13 monitored in a drip-irrigated Maize field at 10 Hz frequency and are averaged over 1, 5, 10,
14 15, 30, 45, 60, and 120 minutes considering daytime unstable conditions. Optimal averaging
15 period to simulate WUE fluxes for each growth stage is obtained by considering cumulative
16 frequency (Ogive) curves. A clear departure of EBR from unity was observed during dough
17 and maturity stages of the crop due to ignorance of canopy heat storage. Deviation in
18 representing water (carbon) fluxes relative to the conventional 30 min average is within $\pm 3\%$
19 ($\pm 10\%$) for 10-120 min averaging and is beyond $\pm 3\%$ ($\pm 10\%$) for other time-averages.
20 Ogive plots conclude that optimal averaging period to represent carbon, water and WUE fluxes
21 is 15-30 min for 6th leaf and silking stages, and is 45-60 min for dough and maturity stages.
22 Dynamics of WUE considering optimal averaging periods are in the range of 1.49 ± 0.95 , 1.37
23 ± 0.74 , 1.39 ± 0.79 , and $3.06 \pm 0.69 \mu\text{mol mmol}^{-1}$ for the 6th leaf, silking, dough, and maturity
24 stages respectively. Error in representing WUE with conventional 30 min averaging is marginal
25 ($< 1.5\%$) throughout the crop period except for the dough stage (12.12%). We conclude that
26 the conventional 30 min averaging of EC fluxes is not appropriate for the entire growth stage.
27 Our findings can help in developing efficient water management strategies by accurately
28 characterizing WUE fluxes from the EC measurements.

29 **Keywords:** Eddy covariance, Maize crop, Time-average, Energy balance ratio, Ogive
30 function, Water use efficiency.

31 **Research Highlights:**

- 32 1. The time-averages that yield the most effective energy balance closure are identified as
33 45 and 60 minutes.
- 34 2. Insufficiently short time-averages such as 1 and 5 minutes, as well as excessively long-
35 time-averages such as 120 minutes, resulted in a high relative error in representing
36 carbon and water fluxes.
- 37 3. The conventional 30-minute averaging period proved to be insufficient in capturing
38 low-frequency fluxes, necessitating the use of longer averaging periods.
- 39 4. Different time averaging periods are to be considered to compute the EC fluxes
40 considering the crop growth stage.

41 **1.0 INTRODUCTION**

42 Water use efficiency (WUE) is an important eco-hydrologic trait relating two important
43 processes of plant metabolism namely carbon fixation (via photosynthesis) and water
44 consumption (via transpiration) (Bramley, 2013). The need for achieving food security with
45 diminishing water resources under changing climate has made WUE as the controlling
46 parameter in planning and design of irrigation strategies (Tang, 2015). Depending on the scale
47 of investigation, WUE can be quantified at: i) leaf, ii) plant, iii) ecosystem, or iv) regional
48 scales (Medrano, 2015). Of these, ecosystem WUE has taken precedence in irrigation and
49 agronomy due to: i) accurate and reliable measurement using micrometeorological techniques,
50 ii) ability to evaluate the role of various water conservation techniques on ecosystem
51 productivity, and iii) understand the relation between carbon and water cycles in response to
52 changes in climate (Tang, 2015; Tong, 2014).

53 Eddy covariance (EC) is a non-destructive, micrometeorological technique for direct
54 measurement of water vapour (H₂O) and carbon (CO₂) fluxes between vegetation and
55 atmosphere at high temporal frequency (Aubinet, 1999; Leclerc and Foken, 2014). EC method
56 precisely measures the overall transfer of heat, mass, and momentum between the earth's
57 surface (such as vegetation) and the atmosphere. This is achieved by estimating the covariance
58 of turbulent fluctuations in vertical wind (referred to as eddies) with respect to the specific flux
59 under consideration such as H₂O, CO₂, temperature. EC represents the scalar fluxes of interest

60 (representative of eco-hydrological processes) from a region upwind of the measurement
61 known as the footprint. At ecosystem scale, WUE is estimated as the ratio of net primary
62 product (NPP: proxy for photosynthesis) to evapotranspiration (ET: proxy for water
63 consumption) (Peddinti, 2020). WUE is a key eco-hydrologic trait that is used to analyse the
64 role of climate change, drought, deficit irrigation, and management strategies on ecosystem
65 productivity. Currently, EC is the most accurate and reliable method for estimating carbon and
66 water exchanges, hence WUE at ecosystem scale (Tong, 2009). A number of studies have
67 demonstrated the efficacy of EC in estimating WUE across a wide range of ecosystems (Tang,
68 2015; Tong, 2014; Wang, 2017). Error sources that affect the accuracy of EC fluxes are
69 grouped into: i) Unrepresentative (due to footprint heterogeneity, unsatisfied underlying
70 theory), ii) Measurement uncertainties (due to random errors, interference and contamination,
71 sensor drifts) and iii) Measurement biases in fluxes (tilt, frequency losses, air density
72 fluctuations etc). Despite improvements in measurement accuracy, data sampling, and
73 processing techniques, EC method still suffers from the drawback of lack of conservation
74 among the energy terms, resulting in energy balance closure (EBC) problem (Charuchittipan,
75 2014; Foken, 2011; Reed, 2018). Lack of EBC as observed in EC system is reported across
76 diverse ecosystems ranging from simple bare soils (Oncley, 2007), to homogeneous grasslands
77 (Twine, 2000), to heterogeneous croplands (Peddinti and Kambhammettu 2019), to complex
78 forest ecosystem (Charuchittipan, 2014; Wilson, 2002). Apart from the errors associated with
79 instrumentation, measurement, and neglected energy sinks, lack of EBC at the EC sites is also
80 attributed to the omission of low frequency secondary circulations in the turbulent flux
81 estimation (Wilson, 2002). This problem can be circumvented by choosing appropriate
82 averaging period during flux estimation, the selection of which is based on: i) ‘ensemble block
83 time-averaging method’ (Finnigan, 2003; Malhi, 2004; Sakai, 2001), and ii) ‘Ogive method’
84 (Berger, 2001).

85 A number of studies have highlighted the importance of averaging period in quantifying
86 the EC fluxes, with an objective to obtain optimal time-averaging period under various canopy
87 and surface roughness conditions. While smaller averaging periods (15-30 min) are suitable
88 for managed croplands, flux estimation from forest and tall canopies demand longer averaging
89 periods (60-120 min) due to the presence of large-sized, slow moving eddies (Finnigan, 2003;
90 Sakai, 2001; Sun, 2006). Zhang (2013) concluded that time-averaging of EC fluxes has to be
91 done in accordance with the observation scale. In an analysis of Chengliu riparian forest in
92 China, they found that lower time-averaging periods (15 min) are suitable for daily variation

93 of EC fluxes, whereas higher time-averaging periods (60 min) are suitable for long-term flux
94 computations. A similar observation was made by Lee (2004) over farmlands. In a wheat field
95 in Yucheng, China, 10 min and 30 min averaging periods were found suitable for diurnal and
96 long-term flux observations respectively. Flux observations over a Maize crop at Daxing
97 experimental station in China conclude that optimal time-averaging period has to be considered
98 in accordance with crop growth stage (Feng, 2017). However, they observed a marginal (< 3
99 %) error in representing the fluxes at conventional 30 min averaging relative to the optimal
100 averaging obtained for each growth stage.

101 Maize is the third most important cereal crop in India after rice and wheat, and accounts
102 for about 10 % of total food production in the country (Sharma, 2018; Ficci 2014). In spite of a
103 huge area under cultivation (9.4 MHa), high production (23 million tons), and enormous water
104 consumption (18 BCM), both crop productivity (2.5 t ha⁻¹) and crop water productivity (CWP)
105 (1.83 kg m⁻³) of Indian Maize are far lower than corresponding world averages (Sharma, 2018).
106 Low CWP (hence, WUE) of Indian Maize can be attributed to: i) a high dependence (85 %) on
107 erratic, uncertain rainfall, ii) low adoption of hybrid varieties, iii) improper drainage facilities
108 leading to water logging, and iv) unscientific application of irrigation water without analysing
109 soil-water-crop interactions (Shankar, 2012). Thus, an accurate quantification of WUE and its
110 temporal variation during the crop cycle is essential for effective irrigation water management
111 of Maize crop (Medrano, 2015).

112 While the effect of time-averaging on carbon and water fluxes measured at EC sites is
113 reported, the effect on their interaction term, i.e. WUE, which is crucial in irrigation water
114 management is unexplored. Evaluation of time-averaging period on WUE dynamics is
115 necessary to understand the contribution of low and high frequency photosynthetic carbon and
116 evaporative water fluxes generated from various field management strategies. Also, most of
117 the EC flux studies are confined to data rich AmeriFLUX, EuroFLUX, and ChinaFLUX sites,
118 with limited focus to Indian fragmented croplands. This motivates the present study, and the
119 objectives of this study are as follows: i) investigate the role of time-averaging of EC fluxes on
120 EBR and WUE dynamics, ii) compute optimal averaging period to simulate carbon and water
121 (hence, WUE) fluxes of Maize crop, and iii) investigate the association of carbon, water, and
122 WUE fluxes between multiple averaging periods. Results of this study can help in designing
123 efficient management strategies using EC datasets in response to changes in WUE during the
124 crop cycle.

125

126 **2.0 MATERIALS AND METHODOLOGY**

127 **2.1 Site Description and Instrumentation**

128 Controlled Maize plots situated at Professor Jaya Shankar Telangana State Agricultural
129 University (PJ TSAU), Hyderabad, Telangana, India (17°19'17" N, 78°24'35" E, 559 m above
130 sea level) forms the study area. The region is composed of red gravel to sandy loam soils with
131 field capacity and wilting point in the ranges of 17.92 - 19.56 % and 8.2 – 9.87% respectively.
132 As per Koppen-Geiger's classification, the region falls under tropical savanna climate zone
133 (Aw) characterized by long dry and short wet seasons (Kottek, 2006). Mean annual
134 precipitation of the region is 900 mm (IMD, 2019) with more than 80% occurring during the
135 monsoon months (Jun-Sep). Temperatures are high during summer (38.33 ± 2.12 °C) and low
136 during winter (30 ± 2.20 °C) months. Humidity of the region varies from 35% in summer to
137 73% in monsoon (CGWB, 2013). Mean seasonal wind speed is in the range of 1.5 to 2.7 m/s
138 (Peddinti and Kambhammettu 2019). Hydro-geologically, the study area forms part of the
139 Deccan plateau characterized by multiple layers of solidified flood basalt resulting from
140 volcanic eruptions. Depth to groundwater ranges from 12 m (pre-monsoon) to 6 m (post-
141 monsoon) (CGWB, 2013).

142 Meteorological parameters and turbulent fluxes were obtained for one crop season, i.e.
143 26 May to 06 Sep, 2019 using an open path eddy covariance (EC) flux tower. The flux system
144 is composed of integrated CO₂/H₂O open-path gas analyzer and 3D sonic anemometer
145 (IRGASON-EB-NC, Campbell Sci. Inc., USA) to measure CO₂ and H₂O concentrations at 3
146 m above the canopy. Raw data was collected with a logger (CR1000, Campbell Sci. Inc., USA)
147 at 10 Hz frequency. Additionally, slow response meteorological variables including
148 precipitation (TE525-L-PTL, Tipping Bucket, Campbell Sci. Inc., USA), soil heat flux
149 (HFP01SC-L-PTL, Campbell Sci. Inc., USA), solar radiation (CNR 4, Campbell Sci. Inc.,
150 USA), and soil moisture (CS616-L-PT-L, Campbell Sci. Inc., USA) were obtained at 10 min
151 intervals.

152

153 **2.2 Data Collection and Processing**

154 Table 1 shows the phenological stages of the Maize crop in the study area (Soujanya,
155 2021). Additionally, leaf-area index (LAI) and mean plant height were monitored during the

156 crop cycle (Table 1). The LAI was measured using the plant canopy analyser, whereas the plant
 157 height was measured using a ruler from the base of the plant to its crown. Maize crops of the
 158 experimental fields are sown on 25th May 2019 and harvested on 6th September 2019 with a
 159 base period of 104 days.

160 **Table 1:** Phenological growth stages and physical properties of the Maize crop

S. No.	Growth stage	Start date	End date	Period Length (days)	Leaf Area Index (m ² m ⁻²)	Plant height (cm)
1	6 th leaf	26/05/2019	12/06/2019	18	0.61	46.8
2	Silking	13/06/2019	19/07/2019	37	1.56	75.2
3	Dough	20/07/2019	12/08/2019	24	3.46	133
4	Maturity	13/08/2019	06/09/2019	25	3.03	134

161

162 Data from the EC system at 10 Hz frequency was converted to ASCII format using
 163 LoggerNet (4.3) software (Campbell Scientific Inc., Logan, Utah, USA), and further
 164 aggregated to various averaging periods (1, 5, 10, 15, 30, 45, 60, and 120 minutes). Post data
 165 processing was done using EddyPro post-processing software (version 7.0.8, LI-COR, USA).
 166 Primary corrections performed on the raw dataset include tilt corrections, turbulent
 167 fluctuations, density fluctuations, frequency corrections and quality checks. Tilt corrections
 168 were made by the double axis rotation method for each averaging period. Either block average
 169 method or linear trending method were considered to compute the turbulent fluctuations. Block
 170 averaging method was used for detrending the fluxes at 1, 5, 10, 30, 45, and 60 min averaging
 171 periods. Longer averaging periods (e.g. 120 min) has resulted in inconsistency in the obtained
 172 fluxes, which is a weakness of the block averaging (Renhua, 2005; Sun et al., 2006). Hence,
 173 linear trend removal method was used to compute the fluxes for 120 min averaging period.
 174 Density fluctuation corrections were done using Webb–Pearman–Leuning (WPL)
 175 method. Quality checks were performed following a flagging policy proposed by Mauder and
 176 Foken (2006) (0-1-2 system). Flag set to "0" corresponds to the best quality fluxes, "1"
 177 corresponds to fluxes acceptable for general analysis, and "2" corresponds to poor quality

178 fluxes that should be removed from the dataset. The resulting fluxes may exhibit spikes,
 179 discontinuity, randomness etc. There is a need to perform secondary corrections on the data
 180 that include flux spike removal (Vickers and Mahrt 1997), friction velocity corrections (to filter
 181 night time observations), gap filling and uncertainty analysis (Finkelstein, 2001), skewness &
 182 kurtosis removal, spectral corrections, and frequency corrections. To correct flux estimates for
 183 low and high frequency losses due to instrument setup, intrinsic sampling limits of the devices,
 184 and various data processing decisions, spectral corrections are performed. Additionally, slow
 185 sensor meteorological data obtained at 1 min interval were processed for different time-
 186 averaging periods using the EddyPro post-processing software (version 7.0.8, LI-COR, USA).
 187

188 **2.3 Effect of time-averaging on EBR and EC fluxes**

189 Violation of law of conservation of energy resulting from the EC observed energy terms
 190 is referred as energy balance closure (EBC). The available energy ($R_n - G$) is generally higher
 191 than the turbulent fluxes ($H + LE$), resulting in a positive balance (Eshonkulov, 2019) where R_n ,
 192 G , H and LE correspond to net radiation, soil heat flux, sensible heat and latent heat
 193 respectively. Apart from instrument and measurement issues, this lack of energy closure is
 194 thought to be partly from averaging periods and coordinate systems (Finnigan, 2003; Finnigan,
 195 2004; Gerken, 2018). The energy closure fraction, commonly termed as energy balance ratio
 196 (EBR) is used to evaluate the quality of EC data by examining energy fluxes at the surface
 197 (Chen and Li 2012), given by:

$$198 \quad EBR = \frac{H + LE}{R_n - G} \quad (1)$$

$$199 \quad H = \rho_a C_p \overline{w' T'} \quad (2)$$

$$200 \quad LE = L_v \overline{w' \rho_v'} \quad (3)$$

201 where ρ_a is the air density; C_p is the specific heat of air, w' is the wind velocity fluctuation, T'
 202 is the temperature fluctuation, L_v is the latent heat of vaporization and ρ_v' is the H₂O gas
 203 concentration fluctuation.

204 EBR helps to determine the averaging period required to calculate H and LE fluxes over a
 205 range of landscapes (Chen and Li 2012). A high EBR ($EBR \geq 0.7$) ensures reliability of EC
 206 observations for use with flux estimation (Barr et al., 2006; Kidston et al., 2010).

207 Eddy fluxes are computed as the covariance between instantaneous deviation in vertical
208 wind speed (w') and scalar component of interest (s') from their respective means, given by

$$209 \quad F \approx \overline{\rho_a w' s'} \quad (4)$$

210 where $\overline{\rho_a}$ is the mean air density, and the overbar represents the time-average of eddy fluxes,
211 which is of interest in the present study. Depending on the scalar component considered (ex:
212 temperature, water vapour (H₂O), carbon dioxide (CO₂) concentration), corresponding eddy
213 fluxes (ex: sensible heat, latent heat, carbon flux) are computed as below.

$$214 \quad F_{CO_2} \approx \overline{\rho_a w' CO_2'} \quad (5)$$

$$215 \quad F_{H_2O} \approx \overline{\rho_a w' H_2O'} \quad (6)$$

216 Ecosystem WUE is then estimated as the ratio of daytime carbon (net primary product) to water
217 fluxes (evapotranspiration), observed considering daytime unstable atmospheric conditions
218 (08:00 am to 04:00 pm) given by:

$$219 \quad WUE = \frac{NPP}{ET} = \frac{F_{CO_2}}{F_{H_2O}} \quad (7)$$

220 Fluxes originating from real-world sites are composed of both high frequency (turbulence) and
221 low frequency (advection) fluctuations, with a spectral gap in between. Isolating local
222 turbulence component for use with flux studies is achieved by choosing an appropriate
223 averaging period, T_1 (typically 30 minutes) on fast response measurements operating at high
224 frequency T_2 (Manon and Kristian 2020). Optimal averaging period (T_1) should be long enough
225 to reduce random error (Berger, 2001) and short enough to avoid non-stationarity associated
226 with advection (Foken & Wichura, 1996). The flux estimates (eq. 2) are further decomposed
227 into frequency dependent contributions, known as co-spectra $Co_{ws}(f)$ between vertical wind
228 velocity (w) and scalar of interest (s) for frequencies ' f ' (Manon and Kristian 2020). For an
229 accurate estimation of the flux, it is essential that the EC method is applied under conditions
230 where the flow is stationary, and all eddies carrying flux are sampled. Given that the flow
231 remains stationary, an 'Ogive' serves as a check for the essential requirement to sample all
232 scales carrying the flux. Ogive function is well proposed to check if all low frequency fluxes
233 are included in the turbulent flux measured with the EC method (Foken & Wichura, 1996;
234 Foken et al., 2005). It is used to investigate the energy balance losses caused by low frequency
235 fluxes. Ogive analysis is performed to investigate the flux contribution from each frequency

236 range and to arrive at most suitable averaging period to capture most of the turbulent fluxes
 237 (Desjardans, 1989; Charuchittipan, 2014). Ogive function thus provides the cumulative sum of
 238 co-spectral energy starting from the highest frequency, given by:

$$239 \quad \text{Og}_{\text{ws}}(f_0) = \int_{f_0}^{\infty} \text{Co}_{\text{ws}}(f) df \quad (8)$$

240 The point of convergence on the Ogive plot to an asymptote corresponds to optimal averaging
 241 period (T_1) for use with averaging of high frequency turbulence fluxes. In other words, the
 242 point at which the Ogive plot flattens out represents the optimal averaging period. A total of
 243 eight averaging periods, i.e., 1, 5, 10, 15, 30, 45, 60, and 120 minutes were considered to
 244 investigate the role of time-averaging on EBR, EC and WUE fluxes, and further to arrive at the
 245 optimum averaging period for use with WUE estimation. The biophysical and physiological
 246 characteristics such as plant height, crop water requirement, LAI, etc. changes with respect to
 247 the crop growth stage (Chintala et al., 2024) and have a significant effect on the EC fluxes.
 248 Since these factors vary over growth stages, time-averaging of EC fluxes is separated based on
 249 crop growth stage.

250

251 **2.4 Performance Evaluation**

252 The ability of various averaging periods to close the energy balance and compute the
 253 EC fluxes is evaluated using three goodness of fit indicators, namely: a) coefficient of
 254 determination (R^2), b) root mean squared error (RMSE), and c) relative error (RE). While R^2
 255 and RMSE aim to quantify the error in closing the energy balance, RE is aimed to compute the
 256 error in estimating EC fluxes with conventional 30 min averaging period relative to optimal
 257 averaging period.

258 Root mean square error (RMSE) measures overall accuracy in closing the energy balance for
 259 a given averaging period by penalizing large errors heavily, given by:

$$260 \quad \text{RMSE} = \left[\frac{\sum_{i=1}^n ((R_n - G)_i - (H + LE)_i)^2}{n} \right]^{0.5} \quad (9)$$

261 where n is the number of observations.

262 Coefficient of determination (R^2) and Pearson correlation coefficient (r) are the measures of
 263 the strength of linear association between turbulent fluxes and available energy, given by:

$$264 \quad R^2 = \left\{ \frac{\sum_{i=1}^n [(R_n - G)_i - \overline{(R_n - G)}]^2 [(H + LE)_i - \overline{(H + LE)}]^2}{\sqrt{\sum [(R_n - G)_i - \overline{(R_n - G)}]^2} \sqrt{\sum [(H + LE)_i - \overline{(H + LE)}]^2}} \right\}^2 \quad (10)$$

$$265 \quad r = \left\{ \frac{\sum_{i=1}^n [(R_n - G)_i - \overline{(R_n - G)}] [(H + LE)_i - \overline{(H + LE)}]}{\sqrt{\sum [(R_n - G)_i - \overline{(R_n - G)}]^2} \sqrt{\sum [(H + LE)_i - \overline{(H + LE)}]^2}} \right\} \quad (11)$$

266 Relative error (RE) provides the disparity in the fluxes estimated with conventional (30 min)
 267 relative to the fluxes estimated with optimal averaging period, given by:

$$268 \quad RE = \left[\frac{F_{opt} - F_{30min}}{F_{opt}} \right] \times 100 \quad (12)$$

269 where F_{opt} and F_{30} are the flux of interest considering optimal and conventional (30 min)
 270 averaging periods.

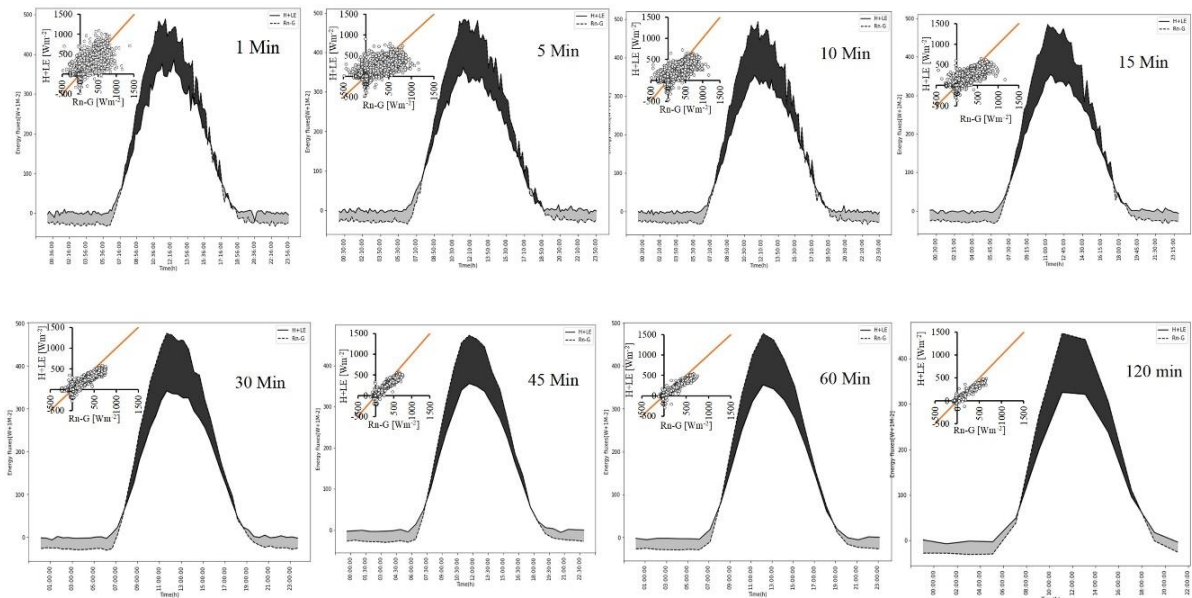
271 Averaging period corresponding to high R^2 (close to 1), low RMSE (close to zero) is considered
 272 to be the optimal choice in representing the EC fluxes.

273

274 3.0 RESULTS AND DISCUSSION

275 3.1 Diurnal variations in energy balance components

276 To understand the energy variation in response to rapid changes in meteorological
 277 conditions, we analysed the diurnal variations in energy balance components. Figure 1 shows



278

279 **Figure 1:** Diurnal variations in energy balance components (available energy: R_n-G and turbulent fluxes:
 280 $H+LE$) during the crop cycle with different averaging periods. Inset: Scatter-plots between the two
 281 datasets.

282 the diurnal variations in available energy (R_n-G) and turbulent fluxes ($H+LE$) averaged over
 283 the crop cycle for various time-averages. The diurnal variations of (R_n-G) and ($H+LE$) are bell-
 284 shaped, with peak occurring at around noon ($480.16 \pm 14.15 \text{ Wm}^{-2}$, $356.23 \pm 18.51 \text{ Wm}^{-2}$)
 285 (Figure 1). The energy balance difference (shaded areas of the figure) is found to be positive
 286 ($76.88 \pm 43.14 \text{ Wm}^{-2}$) during daylight hours (08:00 am to 06:00 pm) and is negative ($-24 \pm$
 287 11.65 Wm^{-2}) for the remaining time. The vertical offset between the two curves, representing
 288 the residual of energy balance is highest around the noon ($142.39 \pm 19.42 \text{ Wm}^{-2}$), and is
 289 consistent between the averaging periods. For an average site-day, the cumulative energy
 290 balance difference was found to be constant with a mean of $1811 \pm 91.56 \text{ Wm}^{-2}$ at all averaging
 291 periods. The cumulative energy balance difference is crossing the ‘zero’ line at around 11:30
 292 am. The variation is rough at lower averaging periods due to a high sample size ($n= 10859$ at
 293 $T = 1 \text{ min}$) and is gradually smoothed towards higher averaging periods ($n= 811$ at $T = 120$
 294 min). The slope of regression lines between ($H+LE$) and (R_n-G) considering all averaging
 295 periods are in the range of 0.59 to 0.71 with a mean of 0.65 ± 0.041 . The intercept is ranged
 296 from 19.01 to 31.56 Wm^{-2} . The best slope (≥ 0.70) and intercept ($\leq 20 \text{ Wm}^{-2}$) were achieved
 297 with 45 and 60 minutes averaging periods, which is consistent with literature (Gao, 2017;
 298 Leuning, 2012). This conclude that, longer averaging periods have a good closure over shorter
 299 averaging periods. The strength of linear association between (R_n-G) and ($H+LE$) around the
 300 best fit line, explained by r is high ($0.80 < r \leq 0.9$) at low averaging periods, i.e., 1, 5, 10
 301 minutes, and is very high ($r > 0.9$) for other averaging periods (Table 2). However, the departure
 302 of the data from 1:1 line is relatively low both at short and long averaging periods. Our findings
 303 show that averaging period has minimal influence in representing the energy balance terms.
 304 However, data scatter around 1:1 line is high for shorter time-averages due to large sample size
 305 and data randomness.

306 **Table 2:** Summary of linear regression parameters in closing the energy balance with different
 307 averaging periods.

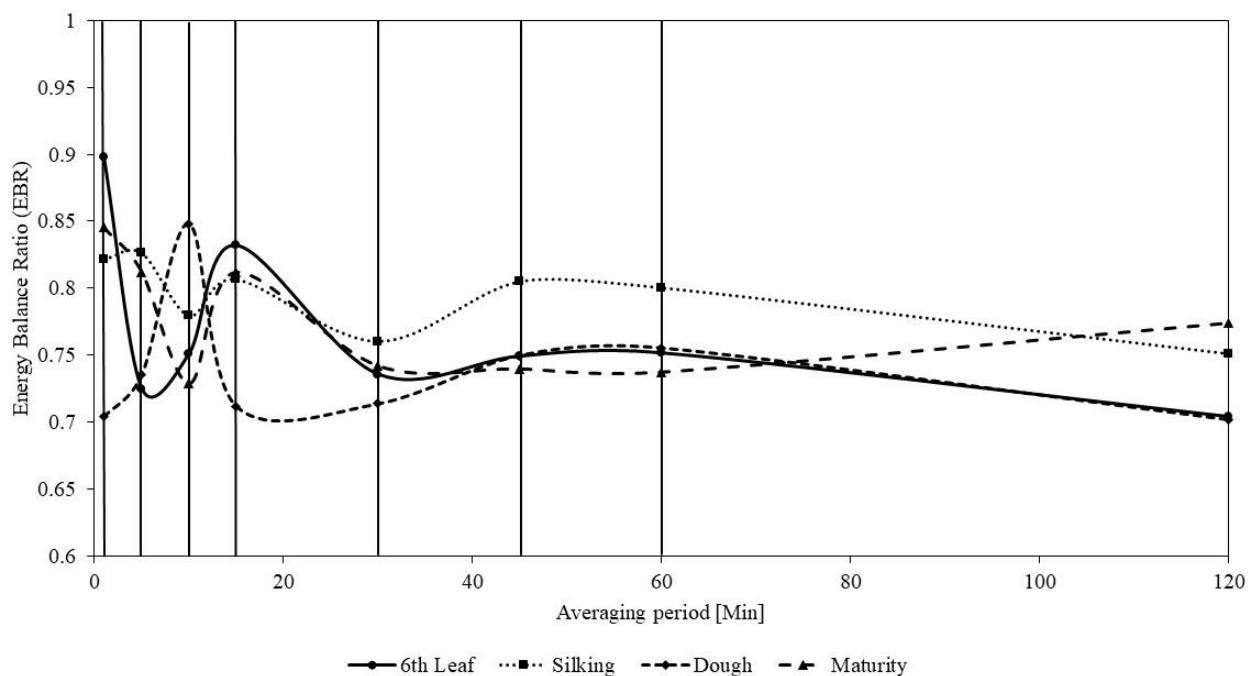
Averaging Period	Slope	R^2	Intercept (Wm^{-2})	r	N	RMSE (Wm^{-2})
1min	0.63	0.66	30.31	0.81	10859	98.38

5min	0.59	0.74	31.56	0.86	10785	76.47
10min	0.60	0.80	28.94	0.90	10753	64.41
15min	0.63	0.84	26.56	0.92	7150	58.18
30min	0.66	0.93	20.49	0.96	3554	38.33
45min	0.70	0.94	19.99	0.97	2355	36.30
60min	0.71	0.94	19.01	0.97	1765	35.07
120min	0.67	0.93	20.77	0.96	811	39.95

308

309 3.2 Effect of averaging period on EBR and EC fluxes

310 The variation in energy balance ratio (EBR) with averaging period for individual
 311 growth stages of the crop is presented in Figure 2. We observed a clear departure of EBR from

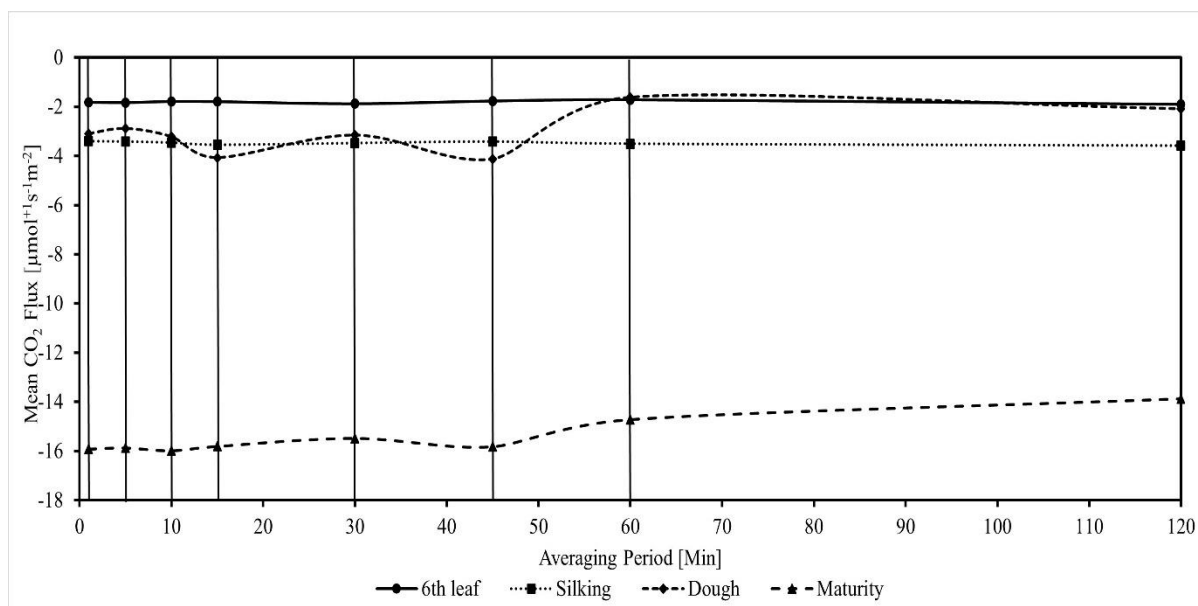


312

313 **Figure 2:** Variation in energy balance ratio (EBR) with averaging period for different growth stages. (Solid
 314 verticals from left to right correspond to the averaging periods of 1 min, 5 min, 10 min, 15 min, 30 min, 45
 315 min, 60 min, and 120 min respectively).

316 unity for all growth stages, particularly with dough and maturity stages due to ignorance of
 317 canopy heat storage. EBR is fluctuating between 0.70 and 0.90 at low (1 – 30 min) averaging

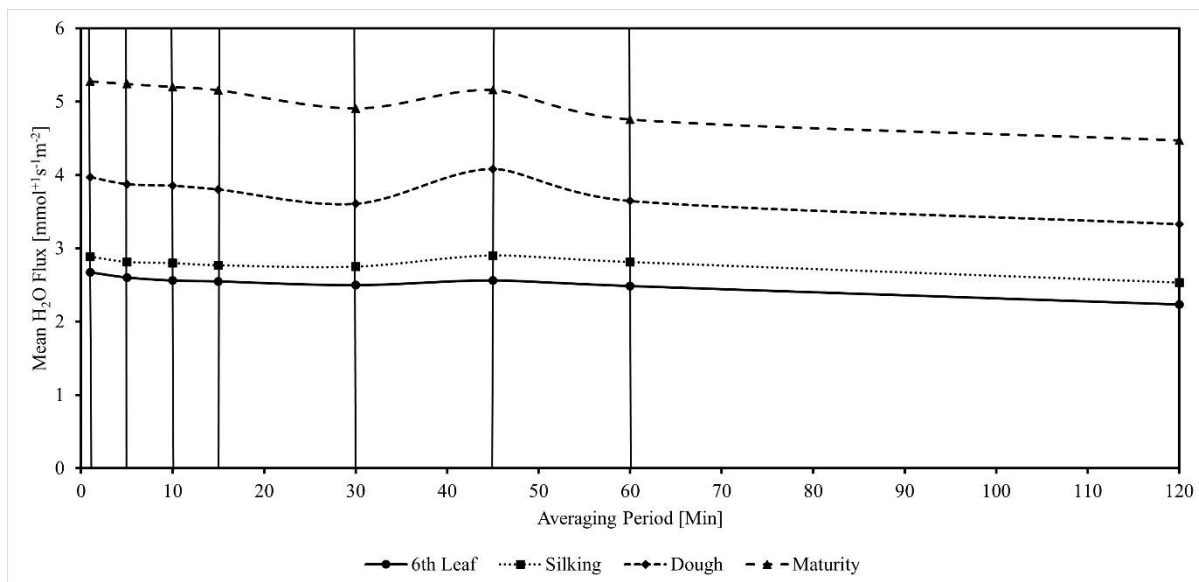
318 periods and is fairly constant (0.75 ± 0.03) at high (≥ 30 min) averaging periods. Our reported
 319 values of EBR during the crop growth are within the typically found range of 0.65 to 1.2 for
 320 most of the crops (Feng, 2017; Finnigan, 2003; Wilson, 2002). The mean EBR with
 321 conventional 30 min averaging period is found to be 0.74, 0.76, 0.71, and 0.74 during 6th leaf,
 322 silking, dough, and maturity stages respectively. Low EBR during the crop cycle can also be
 323 attributed to the ignorance of energy transport associated with large eddies from landscape
 324 heterogeneity. However, EC method assumes the landscape within the footprint of
 325 measurement to be flat and homogenous. This violation might have lowered the EBR. We
 326 could not observe any significant differences in temporal trends of ‘wind speed’ and ‘wind
 327 direction’ between the averaging periods, hence meteorological conditions were not analysed
 328 by varying time-average. Changes in daytime mean carbon and water fluxes with averaging
 329 period for different growth stages of the crop is shown in Figure 3. Carbon fluxes (sink) have
 330 a very low mean ($1.81 \pm 0.06 \mu\text{mol m}^{-2}\text{s}^{-1}$) during 6th leaf stage, low mean during silking (3.48
 331 $\pm 0.07 \mu\text{mol m}^{-2}\text{s}^{-1}$) and dough ($3.03 \pm 0.87 \mu\text{mol m}^{-2}\text{s}^{-1}$) stages, and a high mean (15.44 ± 0.75
 332 $\mu\text{mol m}^{-2}\text{s}^{-1}$) during maturity stage.



333

334 **Figure 3a:** Variation in mean carbon fluxes with averaging period for different growth stages (Solid verticals
 335 from left to right correspond to the averaging periods of 1 min, 5 min, 10 min, 15 min, 30 min, 45 min, 60
 336 min, and 120 min respectively).

337



338

339 **Figure 3b:** Variation in mean water fluxes with averaging period for different growth stages (Solid verticals
 340 from left to right correspond to the averaging periods of 1 min, 5 min, 10 min, 15 min, 30 min, 45 min, 60
 341 min, and 120 min respectively).

342 Mean carbon fluxes during 6th leaf and silking stage are mostly unaffected by averaging period.

343 We observed a gradual increase in water vapour fluxes during the crop cycle from 6th leaf (2.52
 344 $\pm 0.13 \text{ mmol s}^{-1} \text{ m}^{-2}$) to maturity ($5.02 \pm 0.29 \text{ mmol s}^{-1} \text{ m}^{-2}$). As the averaging period is increased,

345 the mean water vapour flux is decreased, with an exception at 45 min averaging period.

346 Deviation in representing carbon and water fluxes at different averaging periods, relative to the

347 conventional 30 min averaging period i.e. relative error (RE) is presented in Figure 4. The RE

348 is obtained by considering daily averages in the deviations for each growth stage. During 6th

349 leaf and silking stages, RE in estimating carbon fluxes is high ($\sim -15 \%$) with low averaging

350 periods, and is gradually diminishing towards higher averaging periods, with an exception at

351 very high (120 min) average period. For dough and maturity stages, RE is found to be

352 significant with higher averaging periods (60-120 min). RE in estimating water vapour fluxes

353 is found to be insignificant at all averaging periods for the 6th leaf and silking stages. However,

354 dough and maturity stages have shown a large variation in RE considering either too-short (1,

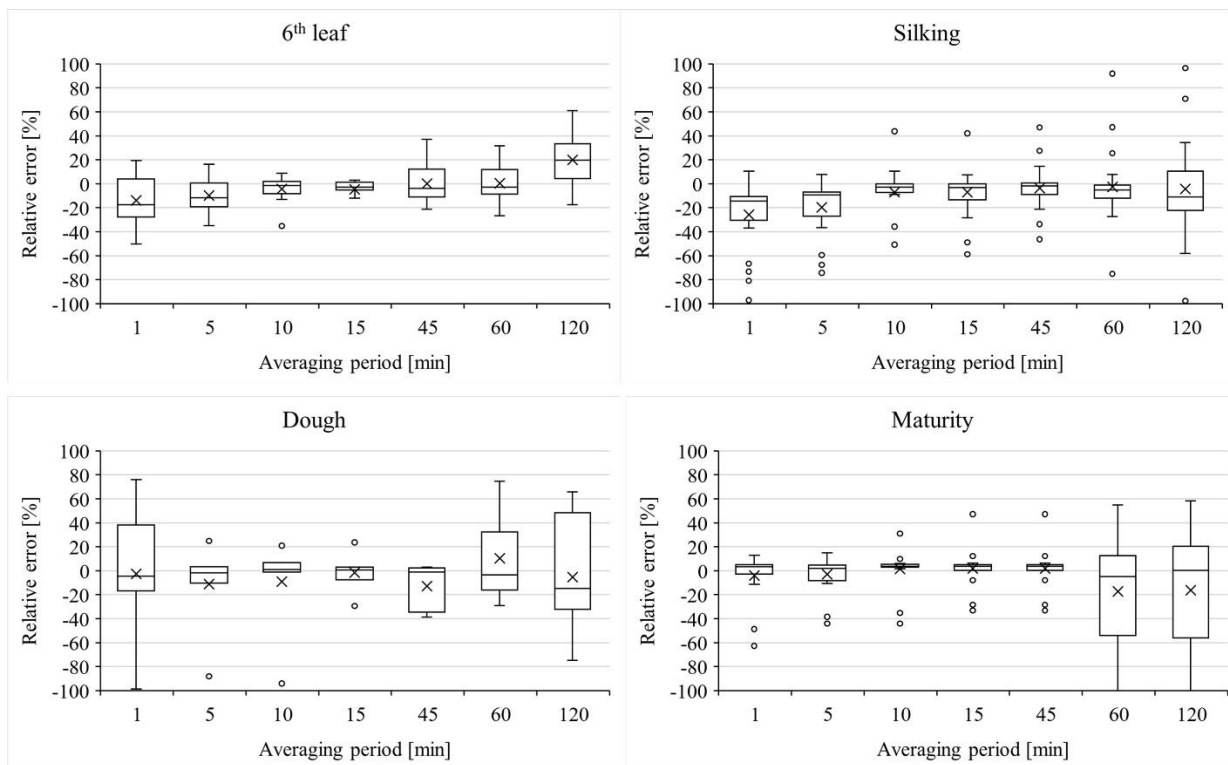
355 5 min) or too-long (60, 120 min) time averages. A high variability in RE for time scales larger

356 than 45 min indicate the effects of sub mesoscale (non-turbulent) motions. Hence, 45 min

357 average period can be considered as optimal in isolating the turbulence components for use

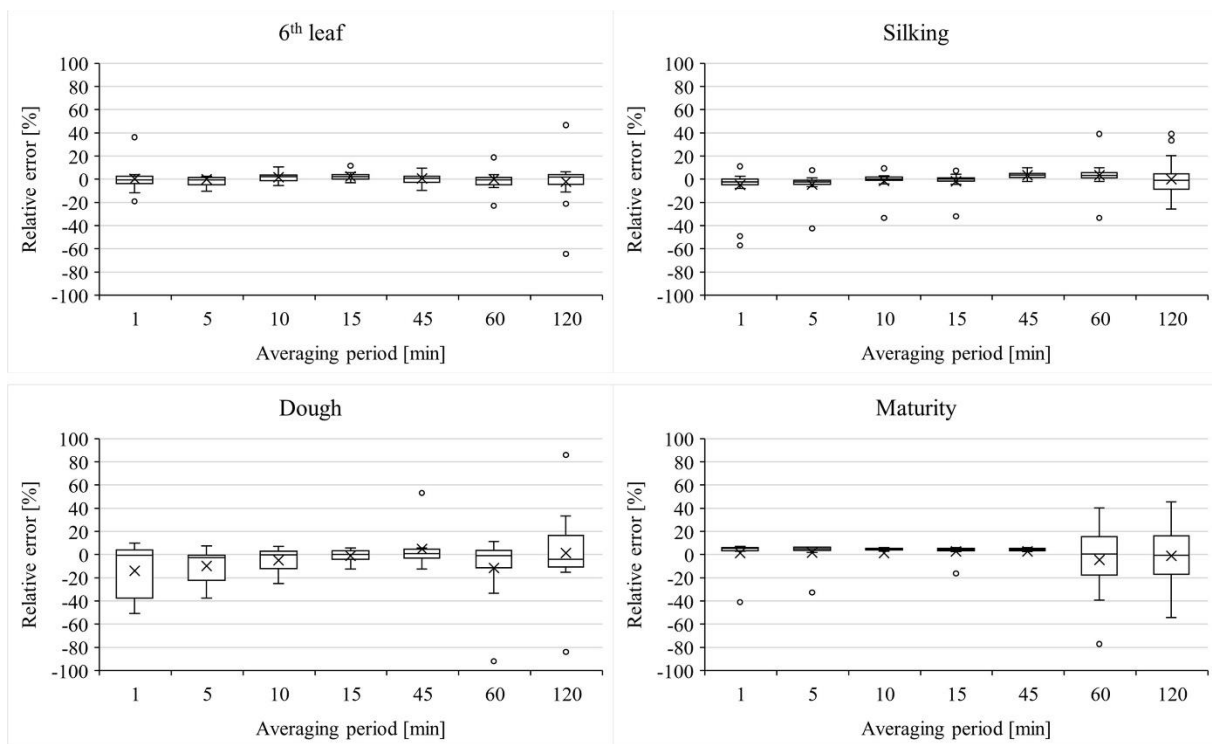
358 with flux representation.

359



360
 361 **Figure 4a:** Whisker plots showing the distribution of error in estimating carbon fluxes with various
 362 averaging periods relative to the conventional 30 min averaging.

363

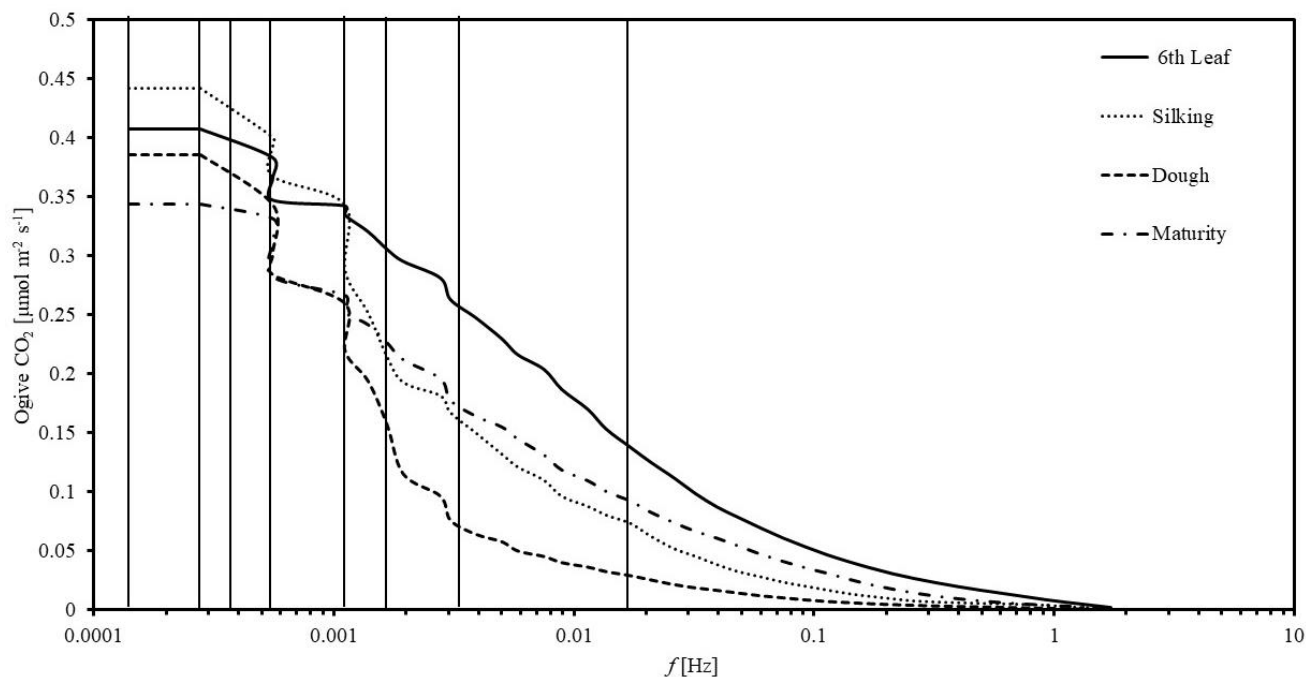


364
 365 **Figure 4b:** Whisker plots showing the distribution of error in estimating water fluxes with various averaging
 366 periods relative to the conventional 30 min averaging.

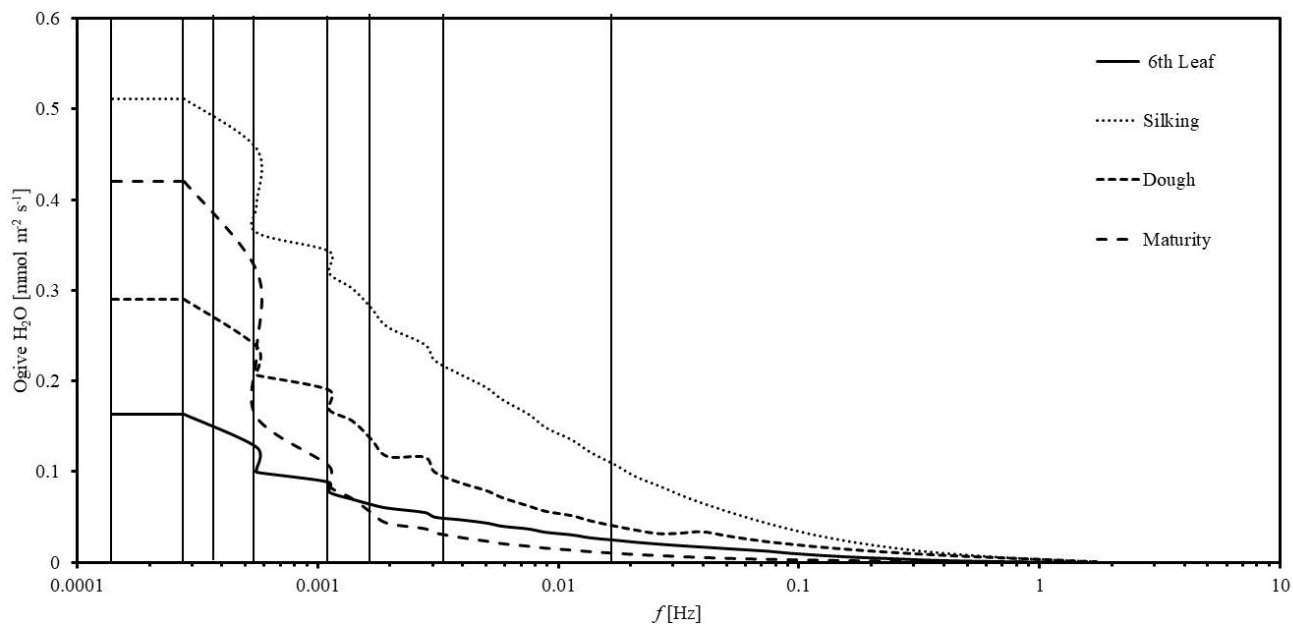
367

368 3.3 Selection of Optimal averaging period

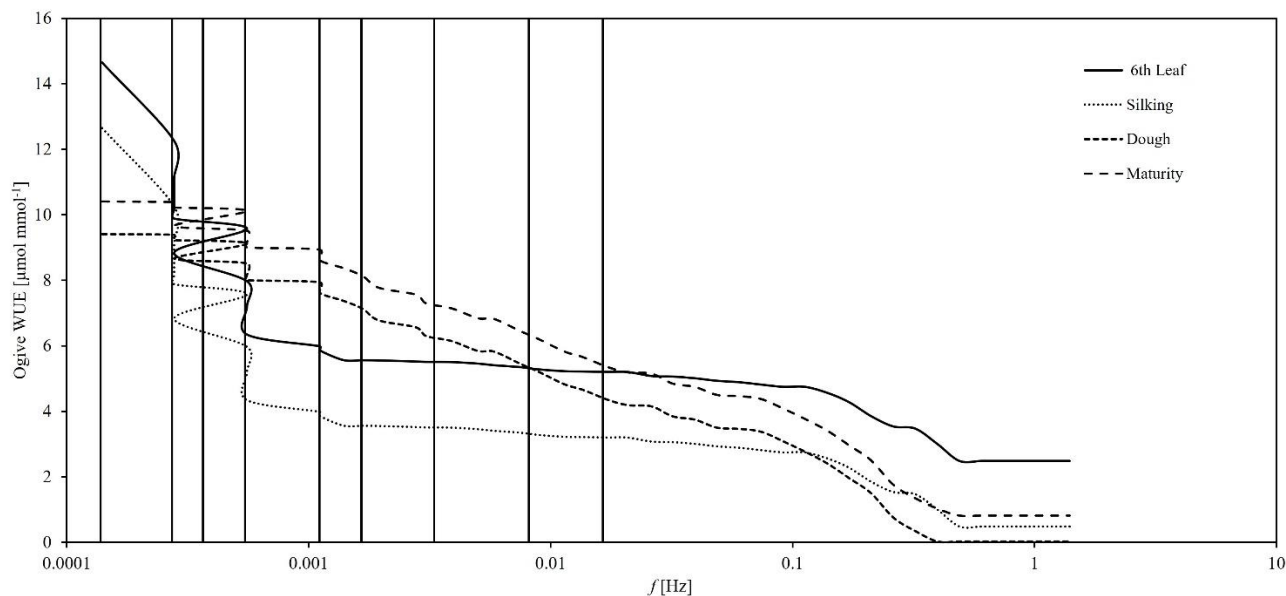
369 Ogive functions representing the cumulative integral of the co-spectral energy starting
 370 with highest frequency, i.e., 0.016 Hz ($T = 1$ min) for carbon, water, and WUE fluxes are
 371 presented



372
 373 **Figure 5a:** Ogive plots of carbon fluxes for different growth stages of the Maize crop. (Solid verticals from
 374 left to right extremes correspond to the averaging periods of 120 min, 60 min, 45 min, 30 min, 15 min, 10
 375 min, 5min and 1 min respectively).



376
 377 **Figure 5b:** Ogive plots of water fluxes for different growth stages of the Maize crop. (Solid verticals from
 378 left to right extremes correspond to the averaging periods of 120 min, 60 min, 45 min, 30 min, 15 min, 10
 379 min, 5min and 1 min respectively)



380

381 **Figure 5c:** Ogive plots of water use efficiency for different growth stages of the Maize crop. (Solid verticals
 382 from left to right extremes correspond to the averaging periods of 120 min, 60 min, 45 min, 30 min, 15 min,
 383 10 min, 5min and 1 min respectively)

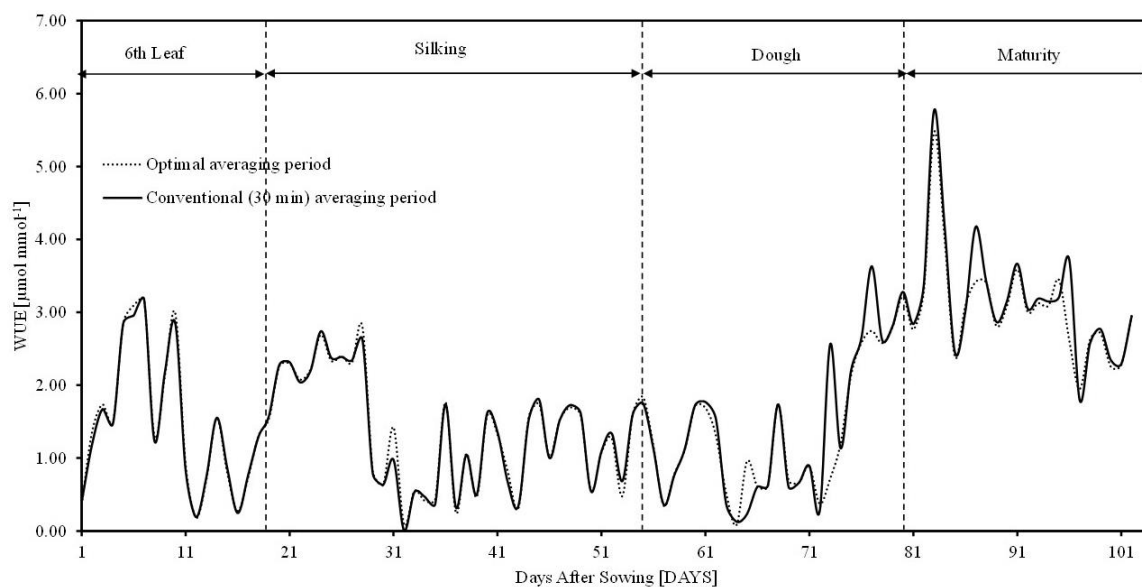
384 in Figure 5. Shorter time periods corresponding to daytime unstable atmospheric conditions
 385 (08:00 am to 04:00 pm) for various growth stages were investigated. Ogive plots of carbon
 386 fluxes for 6th leaf and silking stages showed an increasing trend up to 0.011 Hz (15 min) and
 387 remained fairly constant before 0.0055 Hz (30 min). This concludes that whole turbulent
 388 spectrum can be covered with 15 to 30 min averaging, with negligible flux contribution from
 389 longer frequencies. Ogive plots of carbon fluxes for dough and maturity stages showed a
 390 continuous increasing trend without a defined plateau (horizontal asymptote) in between. This
 391 conclude that the conventional 30 min averaging period is inadequate to capture the low
 392 frequency fluxes, thus demanding for higher averaging periods. We observed a similar
 393 behaviour with water fluxes (Figure 5b). The flat part of the Ogive curve representing the
 394 optimal averaging period was found to vary across the crop cycle. While 15-30 min time-
 395 average is suitable for aggregating the EC fluxes during 6th leaf and silking stages, 45-60 min
 396 averaging is more appropriate for dough and maturity stages. Similar to carbon and water
 397 fluxes, the Ogive plots for WUE were presented in Figure 5c. From this, it is observed that the
 398 flat part of Ogive is achieved at 15 min time average period for the stages of 6th leaf and silking
 399 and 45 min time average for the dough and maturity stages which is similar to the carbon and
 400 water fluxes. It concludes that the WUE followed a similar behaviour as its individual fluxes
 401 i.e. carbon and water fluxes in achieving optimal time averages. The crop biophysical factors
 402 like LAI and plant height are minimum during 6th leaf and silking stages contributes low
 403 quantity of CO₂ and H₂O fluxes (refer figure 3a & 3b) whereas they are maximum in the later

404 stages of the crop i.e., dough and maturity contributing to high quantities of CO₂ and H₂O
 405 fluxes (refer figure 3a & 3b). Our results are in accordance with the previous studies of Fong
 406 et al., 2020 on Cotton, where the responses in NPP and ET were related seasonally to plant
 407 growth stages. The previous studies on various crops revealed that the NPP and ET fluxes were
 408 initially low in the early stages and increases towards maturity stage due to crop phenology and
 409 management practices. To capture these low quantity fluxes, low averaging periods i.e., 15 min
 410 is sufficient, whereas 45 min time-averaging period can capture high quantity fluxes that are
 411 prevalent during later growth stages of the crop. As the crop characteristics are dependent on
 412 crop growth stages, a single time-averaging period is not appropriate to capture the dynamics
 413 of CO₂ and H₂O fluxes as well their ratio, WUE. This clearly demonstrates that, as the plant
 414 achieves its higher stage, flux contribution from low-frequency components becomes more
 415 valuable. Very low averaging periods (ex: 1 min, 5 min) were found unsuitable to capture low-
 416 frequency flux components, which is in agreement with literature (Feng, 2017).

417

418 3.4 Dynamics of Water use efficiency

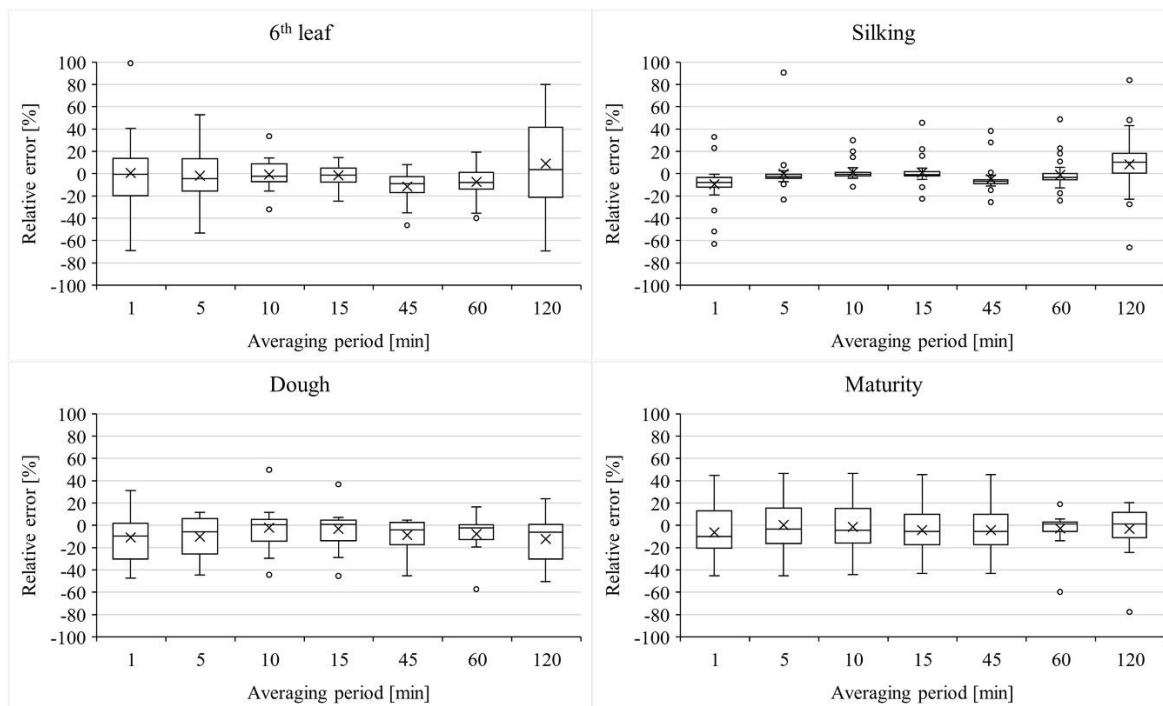
419 Daily means of water use efficiency (WUE) estimated with conventional 30 min and
 420 growth specific optimal averaging periods is presented in Figure 6. Mean WUE fluxes for 6th



421

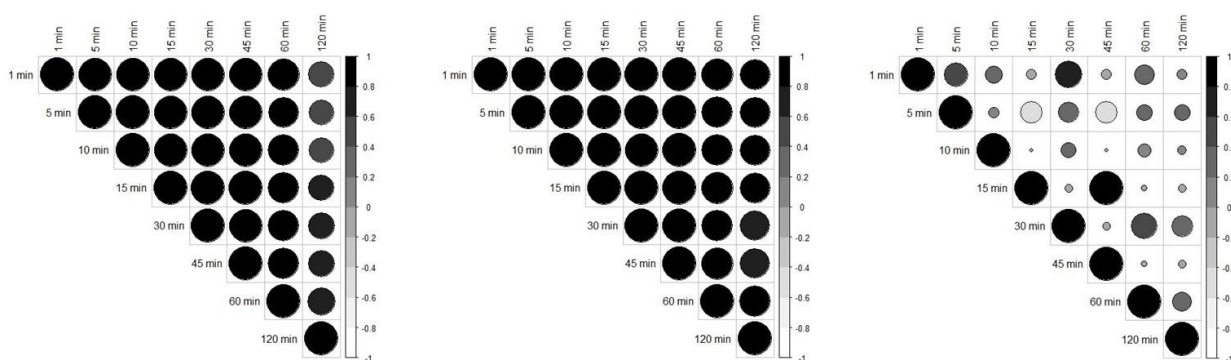
422 **Figure 6:** Seasonal variations in daily mean WUE fluxes obtained with conventional 30 min (solid) and
 423 optimal averaging periods (dotted) during the crop cycle.

424 leaf, silking, dough and maturity stages with conventional 30 min averaging are 1.48 ± 0.96 ,
425 1.36 ± 0.73 , 1.38 ± 0.95 and $3.184 \pm 0.78 \mu\text{mol mmol}^{-1}$ respectively. Corresponding fluxes
426 with stage specific optimal averaging periods are 1.49 ± 0.95 , 1.37 ± 0.74 , 1.39 ± 0.79 and 3.06
427 $\pm 0.69 \mu\text{mol mmol}^{-1}$ respectively. Error in estimating mean daily WUE fluxes with 30 min
428 averaging is very low ($< 1.45\%$) during 6th leaf and silking stages, low (8.56 to 9.04 %) during
429 maturity stage, and is moderate (11.84 to 12.12 %) during dough stage. This conclude that,
430 choice of optimal averaging period is more crucial for late stage growth periods of the crop.
431 Distribution of error in estimating WUE fluxes with various averaging periods relative to
432 conventional 30 min average period (RE) is presented in Figure 7. A close to zero RE with all
433 averaging periods during 6th leaf and silking stages conclude that, choice of averaging period
434 has insignificant role in estimating the WUE fluxes, particularly during early growth stages. A
435 slightly high RE ($\sim -5.4\%$) during dough and maturity stages conclude that, choice of averaging
436 period matters for WUE estimation during late stage periods. Hence, conventional 30 min
437 averaging period can be considered for estimating WUE fluxes during 6th leaf and silking
438 stages, whereas optimal averaging period need to be considered for estimating WUE fluxes
439 during dough and maturity stages. Correlation charts showing the linear association within
440 carbon, water, and WUE fluxes represented at different averaging periods is presented in Figure
441 8. For ease with comparison, data for the entire crop cycle was considered. Linear association
442



443
 444 **Figure 7:** Whisker plots showing the distribution of error in estimating WUE fluxes with various averaging
 445 periods relative to the conventional 30 min averaging.

446 between any two averaging periods is positive ($\rho > 0.56$) for carbon and water fluxes. Except
 447 with 120 min time-averaging, all other averaging periods are strongly correlated ($\rho > 0.87$)
 448 with 30 min averaging period. However, a poor linear association in WUE fluxes was observed
 449 between any two averaging periods, which is attributed to a larger variation in individual WUE
 450 fluxes between averaging periods. However, the corresponding individual carbon and water
 451 fluxes have recorded low variations between time averages. This conclude that, the need for
 452 optimal averaging period is more crucial in estimating WUE fluxes rather than individual
 453 carbon and water fluxes. Our findings can improve representation of WUE fluxes using EC
 454 data, thereby help in developing efficient water management strategies in response to WUE
 455 changes.



457 **Figure 8:** Correlation charts showing the linear association of **a)** Carbon fluxes, **b)** Water fluxes, and **c)**
 458 WUE fluxes estimated with different averaging periods.

459

460 **4.0 CONCLUSIONS**

461 This study explores the effect of averaging period of EC fluxes on EBR dynamics and
 462 WUE in semi-arid Indian conditions. The proposed methodology was applied on drip-irrigated
 463 Maize field for one crop period (May-Sept 2019). Major findings of this study are:

- 464 • EBR was found vary marginally at low averaging periods and less significant during
 465 higher averaging periods.
- 466 • With reference to conventional 30 min averaging period, relative error is within 12%
 467 for 10-45 min averaging periods for carbon fluxes and is within 5% for 15-45 averaging
 468 periods for water fluxes.
- 469 • From Ogive analysis we found the optimal averaging period as 15 - 30 min for the 6th
 470 leaf, and silking stages, and as 45 – 60 min for the dough and maturity stages.
- 471 • The mean carbon fluxes are increasing from $1.81 \pm 0.06 \mu\text{mol}^+\text{m}^{-2}\text{s}^{-1}$ (6th leaf stage)
 472 to $15.44 \pm 0.75 \mu\text{mol}^+\text{m}^{-2}\text{s}^{-1}$ (maturity stage) which indicates that carbon sink is a
 473 function of crop growth period. In case of water fluxes, it increased from 2.52 ± 0.13
 474 $\text{mmol}^+\text{m}^{-2}\text{s}^{-1}$ (6th leaf stage) to $5.02 \pm 0.29 \text{mmol}^+\text{m}^{-2}\text{s}^{-1}$ (maturity stage). Variation of
 475 carbon and water fluxes are directly influencing WUE dynamics.
- 476 • The variation in WUE was increased subsequently with the plant growth and achieved
 477 its maximum value of $5.17 \mu\text{mol mmol}^{-1}$ in between dough to maturity stages which
 478 concludes that, crop consumes more carbon than water as the crop period progresses.
- 479 • The correlation between CO_2 and H_2O fluxes for all averaging periods was found to be
 480 high. However, WUE, which is calculated as the ratio of CO_2 and H_2O fluxes, is not
 481 following the same pattern. While 45 min and 15 min averaged WUE exhibits a good
 482 correlation, 30 min averaged WUE is not correlated with other averaging periods.
 483 Averaging period is found to be an influencing factor in controlling WUE, hence should
 484 be considered with caution during the crop growth.

485 This study is limited to understand the role of different time-averaging periods on EC observed
 486 carbon, water fluxes as well as EC derived WUE fluxes contributed by homogeneous Maize
 487 crop which is having relatively smaller flux footprint in an unstable atmospheric condition.

488 Study findings can help to accurately characterise WUE of Maize crop considering growth
489 stages for effective implementation of irrigation strategies.

490

491 **Acknowledgments**

492 The authors acknowledge the anonymous reviewers for their insightful comments. This
493 research evolved as an extension of a term project in CE6520-Irrigation Water Management
494 course at IIT Hyderabad.

495

496 **Data Availability Statement:**

497 All footprint climatologies, site-level data files, and supplementary material can be accessed
498 via the Zenodo Data Repository (<https://zenodo.org/badge/latestdoi/528291820>)
499 (Shweta07081992, 2022)

500

501 **Author Contribution:**

502 **Arun Rao Karimindla:** Data processing and Analysis, Writing- Original draft. **Shweta**
503 **Kumari:** Conceptualization, Methodology, Project Supervision. **Saipriya SR:** Data processing
504 Analysis, and Writing- Original draft. **Syam Chintala:** Data processing and Analysis, Writing-
505 Original draft. **BVN Phanindra Kambhammettu:** Project Administration, Writing-
506 Reviewing and Editing.

507

508 **Competing interests:**

509 The authors declare that they have no known competing interests or personal relationships that
510 could have appeared to influence the work reported in this paper.

511

512 **5.0 REFERENCES**

513 Barr, A. G., Morgenstern, K., Black, T. A., McCaughey, J. H., & Nesic, Z. (2006). Surface
514 energy balance closure by the eddy-covariance method above three boreal forest stands
515 and implications for the measurement of the CO₂ flux. *Agricultural and Forest*
516 *Meteorology*, 140(1–4), 322–337. <https://doi.org/10.1016/j.agrformet.2006.08.007>

517 Bramley, H., Turner, N. C., & Siddique, K. H. M. (2013). Water Use Efficiency. In C. Kole

- 518 (Ed.), *Genomics and Breeding for Climate-Resilient Crops: Vol. 2 Target Traits* (pp.
519 225–268). Springer Berlin Heidelberg. https://doi.org/10.1007/978-3-642-37048-9_6
- 520 Berger, B. W., Davis, K. J., Yi, C., Bakwin, P. S., & Zhao, C. L. (2001). Long-term carbon
521 dioxide fluxes from a very tall tower in a northern forest: Flux measurement
522 methodology. *Journal of Atmospheric and Oceanic Technology*, 18(4), 529–542.
- 523 Central Ground Water Board. (2015). Annual Report 2013.
524 https://cgwb.gov.in/old_website/Annual-Reports/Annual-Report-2013-14.pdf
- 525 Charuchittipan, D., W. Babel, M. Mauder, J. P. Leps, and T. Foken, 2014: Extension of the
526 Averaging Time in Eddy-Covariance Measurements and Its Effect on the Energy
527 Balance Closure. *Boundary-Layer Meteorol.*, **152**, 303–327,
528 <https://doi.org/10.1007/s10546-014-9922-6>.
- 529 Chen, Y. Y., and M. H. Li, 2012: Determining adequate averaging periods and reference
530 coordinates for eddy covariance measurements of surface heat and water vapor fluxes
531 over mountainous terrain. *Terr. Atmos. Ocean. Sci.*, **23**, 685–701,
532 [https://doi.org/10.3319/TAO.2012.05.02.01\(Hy\)](https://doi.org/10.3319/TAO.2012.05.02.01(Hy)).
- 533 Chintala, S., Karimindla, A. R., & Kambhammettu, B. V. N. P. (2024). Scaling relations
534 between leaf and plant water use efficiencies in rainfed Cotton. *Agricultural Water*
535 *Management*, 292, 108680. <https://doi.org/10.1016/j.agwat.2024.108680>
- 536 Desjardins, R. L., MacPherson, J. I., Schuepp, P. H., & Karanja, F. (1989). An evaluation of
537 aircraft flux measurements of CO₂, water vapor and sensible heat. *Boundary-Layer*
538 *Meteorology*, 47(1), 55–69. <https://doi.org/10.1007/BF00122322>
- 539 Eshonkulov, R., and Coauthors, 2019: Evaluating multi-year, multi-site data on the energy
540 balance closure of eddy-covariance flux measurements at cropland sites in southwestern
541 Germany. *Biogeosciences*, **16**, 521–540, <https://doi.org/10.5194/bg-16-521-2019>.
- 542 Feng, J., B. Zhang, Z. Wei, and D. Xu, 2017: Effects of Averaging Period on Energy Fluxes
543 and the Energy-Balance Ratio as Measured with an Eddy-Covariance System.
544 *Boundary-Layer Meteorol.*, **165**, 545–551, <https://doi.org/10.1007/s10546-017-0284-8>.
- 545 Ficci, 2014: Maize in India. *India Maize Summit '14*, 1–32.
- 546 Finkelstein, P. L., & Sims, P. F. (2001). Sampling error in eddy correlation flux
547 measurements. *Journal of Geophysical Research*, 106, 3503–3509.

- 548 <https://api.semanticscholar.org/CorpusID:128980052>
- 549 Finnigan, J. J., 2004: A re-evaluation of long-term flux measurement techniques part II:
550 Coordinate systems. *Boundary-Layer Meteorol.*, **113**, 1–41,
551 <https://doi.org/10.1023/B:BOUN.0000037348.64252.45>.
- 552 Finnigan, J. J., R. Clement, Y. Malhi, R. Leuning, and H. A. Cleugh, 2003: Re-evaluation of
553 long-term flux measurement techniques. Part I: Averaging and coordinate rotation.
554 *Boundary-Layer Meteorol.*, **107**, 1–48, <https://doi.org/10.1023/A:1021554900225>.
- 555 Foken, T., and B. Wichura, 1996: Tools for quality assessment of surface-based flux
556 measurements. *Agric. For. Meteorol.*, **78**, 83–105, [https://doi.org/10.1016/0168-](https://doi.org/10.1016/0168-1923(95)02248-1)
557 [1923\(95\)02248-1](https://doi.org/10.1016/0168-1923(95)02248-1).
- 558 Foken, T., Göockede, M., Mauder, M., Mahrt, L., Amiro, B., & Munger, W. (2005). Post-
559 Field Data Quality Control BT - Handbook of Micrometeorology: A Guide for Surface
560 Flux Measurement and Analysis (X. Lee, W. Massman, & B. Law, Eds.; pp. 181–208).
561 Springer Netherlands. https://doi.org/10.1007/1-4020-2265-4_9
- 562 Foken, T., M. Aubinet, J. J. Finnigan, M. Y. Leclerc, M. Mauder, and K. T. Paw U, 2011:
563 Results of a panel discussion about the energy balance closure correction for trace gases.
564 *Bull. Am. Meteorol. Soc.*, **92**, <https://doi.org/10.1175/2011BAMS3130.1>.
- 565 Fong, B. N., Reba, M. L., Teague, T. G., Runkle, B. R. K., & Suvočarev, K. (2020). Eddy
566 covariance measurements of carbon dioxide and water fluxes in US mid-south cotton
567 production. *Agriculture, Ecosystems and Environment*, 292.
568 <https://doi.org/10.1016/j.agee.2019.106813>
- 569 Gao, Z., H. Liu, G. G. Katul, and T. Foken, 2017: Non-closure of the surface energy balance
570 explained by phase difference between vertical velocity and scalars of large atmospheric
571 eddies. *Environ. Res. Lett.*, **12**, <https://doi.org/10.1088/1748-9326/aa625b>.
- 572 Gerken, T., and Coauthors, 2018: Investigating the mechanisms responsible for the lack of
573 surface energy balance closure in a central Amazonian tropical rainforest. *Agric. For.*
574 *Meteorol.*, **255**, 92–103, <https://doi.org/10.1016/j.agrformet.2017.03.023>.
- 575 Kidston, J., Brümmer, C., Black, T. A., Morgenstern, K., Nesic, Z., McCaughey, J. H., &
576 Barr, A. G. (2010). Energy balance closure using eddy covariance above two different
577 land surfaces and implications for CO₂ flux measurements. *Boundary-Layer*

- 578 Meteorology, 136(2), 193–218. <https://doi.org/10.1007/s10546-010-9507-y>
- 579 Kole, C., 2013: *Genomics and breeding for climate-resilient crops: Vol. 2 target traits*. 1–474
580 pp.
- 581 Kottek, M., J. Grieser, C. Beck, B. Rudolf, and F. Rubel, 2006: World map of the Köppen-
582 Geiger climate classification updated. *Meteorol. Zeitschrift*, **15**, 259–263,
583 <https://doi.org/10.1127/0941-2948/2006/0130>.
- 584 Leclerc, M. Y., and T. Foken, 2014: *Footprints in micrometeorology and ecology*. Springer,.
- 585 Lee, X., Q. Yu, X. Sun, J. Liu, Q. Min, Y. Liu, and X. Zhang, 2004: Micrometeorological
586 fluxes under the influence of regional and local advection: A revisit. *Agric. For.*
587 *Meteorol.*, **122**, 111–124, <https://doi.org/10.1016/j.agrformet.2003.02.001>.
- 588 Leuning, R., E. van Gorsel, W. J. Massman, and P. R. Isaac, 2012: Reflections on the surface
589 energy imbalance problem. *Agric. For. Meteorol.*, **156**, 65–74,
590 <https://doi.org/10.1016/j.agrformet.2011.12.002>.
- 591 Malhi, Y., K. McNaughton, and C. Von Randow, 2004: Low Frequency Atmospheric
592 Transport and Surface Flux Measurements. 101–118, [https://doi.org/10.1007/1-4020-](https://doi.org/10.1007/1-4020-2265-4_5)
593 [2265-4_5](https://doi.org/10.1007/1-4020-2265-4_5).
- 594 Manon, M., and M. Kristian, 2020: Estimating local atmosphere-surface fluxes using eddy
595 covariance and numerical Ogive optimization. **15**, 21387–21432,
596 <https://doi.org/10.5194/acpd-14-21387-2014>.
- 597 Mauder, M., and T. Foken, 2006: Impact of post-field data processing on eddy covariance
598 flux estimates and energy balance closure. *Meteorol. Zeitschrift*, **15**, 597–609,
599 <https://doi.org/10.1127/0941-2948/2006/0167>.
- 600 Medrano, H., and Coauthors, 2015: From leaf to whole-plant water use efficiency (WUE) in
601 complex canopies: Limitations of leaf WUE as a selection target. *Crop J.*, **3**, 220–228,
602 <https://doi.org/10.1016/j.cj.2015.04.002>.
- 603 Oncley, S. P., and Coauthors, 2007: The energy balance experiment EBEX-2000. Part I:
604 Overview and energy balance. *Boundary-Layer Meteorol.*, **123**, 1–28,
605 <https://doi.org/10.1007/s10546-007-9161-1>.
- 606 Peddinti, S. R., and B. P. Kambhammettu, 2019: Dynamics of crop coefficients for citrus

- 607 orchards of central India using water balance and eddy covariance flux partition
608 techniques. *Agric. Water Manag.*, **212**, 68–77,
609 <https://doi.org/10.1016/j.agwat.2018.08.027>.
- 610 Peddinti, S. R., Kambhammettu, B. V. N. P., Rodda, S. R., Thumaty, K. C., & Suradhaniwar,
611 S. (2020). Dynamics of Ecosystem Water Use Efficiency in Citrus Orchards of Central
612 India Using Eddy Covariance and Landsat Measurements. *Ecosystems*, 23(3), 511–528.
613 <https://doi.org/10.1007/s10021-019-00416-3>
- 614 Reed, D. E., J. M. Frank, B. E. Ewers, and A. R. Desai, 2018: Time dependency of eddy
615 covariance site energy balance. *Agric. For. Meteorol.*, **249**, 467–478,
616 <https://doi.org/10.1016/j.agrformet.2017.08.008>.
- 617 Sakai, R. K., D. R. Fitzjarrald, and K. E. Moore, 2001: Importance of low-frequency
618 contributions to eddy fluxes observed over rough surfaces. *J. Appl. Meteorol.*, **40**, 2178–
619 2192, [https://doi.org/10.1175/1520-0450\(2001\)040<2178:IOLFCT>2.0.CO;2](https://doi.org/10.1175/1520-0450(2001)040<2178:IOLFCT>2.0.CO;2).
- 620 Sharma, B. R., Gulati, Mohan, Gayathri, Manchanda, S., Ray, I., & Amarasinghe, U. (2018).
621 Water Productivity Mapping of Major Indian Crops. NABARD and ICRIER, 4(1), 88–
622 100.
- 623 Shankar, V., C. S. P. Ojha, and K. S. H. Prasad, 2012: Irrigation Scheduling for Maize and
624 Indian-mustard based on Daily Crop Water Requirement in a Semi- Arid Region. **6**,
625 476–485.
- 626 Soujanya, B., B. B. Naik, M. U. Devi, T. L. Neelima, and A. Biswal, 2021: Dry Matter
627 Production and Nitrogen Uptake as Influenced by Irrigation and Nitrogen Levels in
628 Maize. *Int. J. Environ. Clim. Chang.*, 155–161,
629 <https://doi.org/10.9734/ijecc/2021/v11i1130528>.
- 630 Sun, X. M., Z. L. Zhu, X. F. Wen, G. F. Yuan, and G. R. Yu, 2006: The impact of averaging
631 period on eddy fluxes observed at ChinaFLUX sites. *Agric. For. Meteorol.*, **137**, 188–
632 193, <https://doi.org/10.1016/j.agrformet.2006.02.012>.
- 633 Tang, X., Z. Ding, H. Li, X. Li, J. Luo, J. Xie, and D. Chen, 2015: Characterizing ecosystem
634 water-use efficiency of croplands with eddy covariance measurements and MODIS
635 products. *Ecol. Eng.*, **85**, 212–217, <https://doi.org/10.1016/j.ecoleng.2015.09.078>.
- 636 Tong, X., J. Zhang, P. Meng, J. Li, and N. Zheng, 2014: Ecosystem water use efficiency in a

- 637 warm-temperate mixed plantation in the North China. *J. Hydrol.*, **512**, 221–228,
638 <https://doi.org/10.1016/j.jhydrol.2014.02.042>.
- 639 Tong, X. J., J. Li, Q. Yu, and Z. Qin, 2009: Ecosystem water use efficiency in an irrigated
640 cropland in the North China Plain. *J. Hydrol.*, **374**, 329–337,
641 <https://doi.org/10.1016/j.jhydrol.2009.06.030>.
- 642 Twine, T. E., and Coauthors, 2000: Correcting eddy-covariance flux underestimates over a
643 grassland. *Agric. For. Meteorol.*, **103**, 279–300, [https://doi.org/10.1016/S0168-](https://doi.org/10.1016/S0168-1923(00)00123-4)
644 [1923\(00\)00123-4](https://doi.org/10.1016/S0168-1923(00)00123-4).
- 645 Vickers, D., & Mahrt, L. (1997). Quality control and flux sampling problems for tower and
646 aircraft data. *Journal of Atmospheric and Oceanic Technology*, 14(3), 512–526.
647 [https://doi.org/10.1175/1520-0426\(1997\)014<0512:QCAFSP>2.0.CO;2](https://doi.org/10.1175/1520-0426(1997)014<0512:QCAFSP>2.0.CO;2)
- 648 Wang, X., C. Wang, and B. Bond-Lamberty, 2017: Quantifying and reducing the differences
649 in forest CO₂-fluxes estimated by eddy covariance, biometric and chamber methods: A
650 global synthesis. *Agric. For. Meteorol.*, **247**, 93–103,
651 <https://doi.org/10.1016/j.agrformet.2017.07.023>.
- 652 Wilson, K., E. Falge, M. Aubinet, and D. Baldocchi, 2002: DigitalCommons @ University of
653 Nebraska - Lincoln Energy Balance Closure at FLUXNET Sites. *Agric. For. Meteorol.*,
654 223–243.
- 655 Zhang, P., G. Yuan, and Z. Zhu, 2013: Determination of the averaging period of eddy
656 covariance measurement and its influences on the calculation of fluxes in desert riparian
657 forest. *Arid L. Geogr.*, **36**, 401–407.
- 658
- 659